INVESTIGATING THE PROCESSES THAT CONTROL WATER CHEMISTRY DURING REFILLING OF LAKE NGAMI IN SEMIARID NORTHWEST BOTSWANA

By

SCOTT D. MEIER

Bachelor of Science in Geology

Arkansas Tech University

Russellville, AR

2012

Submitted to the Faculty of the
Graduate College of the
Oklahoma State University
in partial fulfillment of
the requirements for
the Degree of
MASTER OF SCIENCE
May, 2014

INVESTIGATING THE PROCESSES THAT CONTROL WATER CHEMISTRY DURING REFILLING OF LAKE NGAMI IN SEMIARID NORTHWEST BOTSWANA

Thesis Approved:

Dr. Eliot Atekwana

Thesis Adviser

Dr. Tracy Quan

Dr. Joseph Donoghue

ACKNOWLEDGEMENTS

I thank the National Science Foundation for partial funding of this project under the International Research Experience for Students (IRES) initiative. I thank the University of Botswana for providing logistical support for fieldwork and the government of Botswana (Ministry of Education) for providing research permits. Additionally, this work could not have been completed without the financial support of the Boone Pickens School of Geology.

I acknowledge Dr. Loago Molwalefhe for his mentoring and field support while conducting research in Botswana, as well as the incredible group of students who were my research partners in the field: Wes Rutelonis, Eryk Mokganedi, Karabo Kauhanda, and Sheri Gares.

I thank my committee members Dr. Tracy Quan and Dr. Joseph Donoghue who were both extremely generous with their knowledge and time, as well as my advisor Dr. Eliot Atekwana who provided constant guidance and advice over the past two years.

Finally, I thank my family and friends for their constant support throughout my graduate education, and all of my other endeavors.

Name: Scott Meier

Date of Degree: May, 2014

Title of Study: INVESTIGATING THE PROCESSES THAT CONTROL WATER CHEMISTRY DURING REFILLING OF LAKE NGAMI IN SEMIARID NORTHWEST BOTSWANA

Major Field: Geology

Abstract: Lake Ngami is an endorheic lake in the distal portion of the Okavango Delta in semiarid Botswana. The lake was dry until 2009 when it began filling with water. The physical, chemical, and stable isotopic composition of the lake water was documented in order to evaluate the processes that control water properties, and establish baseline values for future temporal and spatial comparisons. Field measurements were made and water samples were collected 25 cm below the surface along a ~18 km axial transect from the inflow river to the distal end of the lake. The major ionic concentrations (e.g., Cl^-, Na^+ Ca^{2+}) and the stable isotope ratios of oxygen ($\delta^{18}O$) and hydrogen (δD) showed three distinct regions of increasing concentrations and isotopic enrichment, respectively along the transect. The $\delta\ ^{18}O$ vs. δD data plot along the Okavango Delta evaporation line and suggest modification of lake chemistry by evaporation. Because the lake's inflow showed little chemical and isotopic variation over the past three years, it is possible that the increased ionic concentrations in lake water are due to evapoconcentration and that the segmentation of major solutes, $\delta^{18}O$, and δD into three regions along the transect, is a result of differential evaporation of lake recharge from 2010, 2011 and 2012, and are thus controlled by the residence time of recharge in the lake. Unlike the major ions, the dissolved inorganic carbon (DIC) concentrations and the stable carbon isotopic ratios ($\delta^{13}C_{DIC}$) increase along the transect to about midway in the lake, and then reach steady state. Carbon cycling in the lake is controlled by evaporation and equilibration between carbon in DIC and atmospheric $CO_{2(g)}$. The results show the importance of evaporation and residence time in controlling the solute chemistry and the dominance of the atmospheric $CO_{2(g)}$ in controlling the carbon isotopic signature during the filling stage of an endohreic lake in an arid environment.

TABLE OF CONTENTS

LIST OF TABLES

Table Page

LIST OF FIGURES

Figure Page

CHAPTER I

INTRODUCTION

Surface water in arid regions is important to the functioning of aquatic ecosystems and for water supply. This is especially true in the middle Kalahari Desert of northwest Botswana where rainfall is low and averages 450 mm/year (Mackay et al., 2011). In this region, the annual flooding of the Okavango Delta is necessary for the preservation of pristine wildlife habitat of the Okavango swamp and also supports the local economy through tourism (Kgathi et al., 2006). Recent variations in regional climate have caused the Okavango Delta to receive more inflow water, which has resulted in hydrologic shifts within the delta causing the formation of new water courses which pool to the surface forming lakes in the Okavango Delta region (Gaughan and Waylen, 2012; Wolski et al., 2014). The quality of newly pooled water is of critical importance, as it will support new ecosystems and may be used for potable water supply.

Lake Ngami in northwest Botswana is an endohreic lake basin located at the southeast distal edge of the Okavango Delta (Fig. 1). Hydrological controls that affect filling and drying of Lake Ngami and other lakes in the region center around seasonal flooding of the Okavango Delta by discharge from catchments in the subtropical Angolan highlands (McCarthy and Ellery, 1998), as well as the changing allocation of water to the

distributaries that flow into the lakes (Shaw et al., 2003; Wolski et al., 2014). Periodic shifts in both climate and hydrologic changes within the Okavango Delta have caused Lake Ngami to alternate between filling and drying cycles throughout its existence. However, the lake has remained mostly dry for the majority of the twentieth century (Grove, 1969; Shaw, 1985; Shaw et al., 2003). Recently, Lake Ngami has begun to fill due to consecutive years of record high flood discharges and redistribution of water of the Okavango River to distributaries in the western portions of the Okavango Delta (Wolski and Murrary-Hudson, 2006; Wolski et al., 2014). Both changes have allowed the lakes in the region to receive a greater volume of inflow than what is annually lost from evaporation and infiltration. We expect both internal and external processes to alter the water properties in Lake Ngami as it continues to fill. Evaporation, transpiration, and mineral dissolution are major influences on the salinization of water bodies in arid environments (Huang and Pang, 2012) and are the processes of primary concern in the water cycling of Lake Ngami. Salinization of ephemeral lakes occurs in the Okavango Delta region and is exemplified by the Makgadikgadi Pans located to the southeast of Lake Ngami. Sua Pan (20°33'0"S, 26°16'48"E), a sub-pan of the Makgadikgadi Pans complex, is characterized by highly saline pools resulting from evaporation of flood discharge, mostly from the Nata River that drains the area east of the Makgadikgadi (Eckardt et al., 2008).

There is a lack of information on the chemical properties of Lake Ngami before its complete drying in the recent past, and therefore no way to assess the history of water quality in the lake. Considering the past cyclicity of filling and drying, Lake Ngami is likely to dry again. Therefore, documenting the chemistry of the lake water during filling

will provide a snapshot of the processes controlling the chemistry of a filling lake in an arid environment. Such information will serve as the background for assessing water quality and its relationship to dynamic chemical processes during the filling cycles of Lake Ngami as well as other lakes in arid environments. The objectives of this study are to assess the chemical evolution of the lake water relative to its source water and to determine the role of evaporation, degradation of drowned vegetation, and the cycling of carbon in altering lake water chemistry. In addition, baseline data will be generated for future assessment of water quality and lacustrine processes.

CHAPTER II

REVIEW OF LITERATURE

Lake Ngami (20°30'7.28"S, 22°44'46.76"E) is located in a depression in the southeast distal portion of the Okavango Delta in northwest Botswana (Fig. 1). The Okavango Delta is a low gradient alluvial fan system formed within the nascent Okavango Rift Zone (Modisi, 2000; Laletsang et al., 2006; Kinabo et al., 2007; 2008; Bufford et al., 2012), and is the largest wetland in southern Africa (McCarthy and Ellery, 1998). The distal portion of the Okavango Delta is comprised of a network of distributary channels that terminate against the Kunyere and Thamalakane faults, a border fault system (Kinabo et al., 2007; 2008, Bufford et al., 2012) that is responsible for the development of the lake basin (e.g., McCarthy et al., 1993).

The Okavango Delta and Lake Ngami are located in a semi-arid environment. Their hydrology is controlled by local rainfall and inflow of water into the Okavango Delta from subtropical watersheds in southern Angola. The low annual average precipitation of 450 mm/year (Mackay et al., 2011) is considered insignificant in the long term hydrology of the delta as evaporation almost always exceeds precipitation throughout the year (Sutcliffe and Parks, 1989). The influx of water from the Okavango

River occurs as an annual flood pulse that arrives during the southern hemisphere winter months and is out of phase with the local rainy season (e.g., Gieske, 1997). The progressive temporal flooding of the Okavango Delta from the proximal portion in Mohembo to the distal portion in Maun (Fig. 1), occurs over a four to six month period (McCarthy and Ellery, 1998). Studies suggest that while the flood pulse is in transit, evapotranspiration is responsible for up to 97% loss of the Okavango River discharge between the proximal and distal portion of the Okavango Delta (Anderson et al., 2003). As a result, the chemical evolution of river water is dominated by evapotranspiration processes, and is characterized by downriver increases in solute concentrations (Sawula and Martins, 1991; Krah et al., 2006; Bauer-Gottwein et al., 2007; Mackay et al., 2011; Mmualefe and Torto, 2011; Akoko et al., 2013) and the enrichment of stable hydrogen and oxygen isotopes (Dincer et al., 1979; Akoko et al., 2013).

Over the past century, flooding of Lake Ngami has been confined to the eastern portion of its 3000 km^2 basin (Grove, 1969; Shaw et al., 2003). Analyses of shoreline deposits have shown that a much more extensive body of water existed in the late Pleistocene which linked the current Lake Ngami basin to the Mababe basin (18°49'3.60"S, 24°14'4.72"E) on the northeastern fringe of the Okavango Delta (Grove, 1969; Shaw, 1988; Shaw et al., 2003; Huntsman-Mapila et al., 2006). Archeological evidence of settlements combined with stratigraphic analysis suggests that a large lake was present during much of the Holocene (Robbins et al., 1998; Robbins et al., 2009). In the time of written history, the lake was chronicled by European explorers who noted depths of up to 13 m (Shaw et al., 2003). Combined records of the explorers also document the narrative of the filling and drying cycles of Lake Ngami from the late

nineteenth century through the twentieth century, during which time the lake has remained mostly dry with intermittent filling years (Stigand, 1912; Stigand, 1923; Shaw, 1985).

Due to consecutive seasons of high rainfall in the catchment area, and redistribution of flow to more western distributaries of the Okavango Delta (Wolski and Murray-Hudson, 2006; Wolski et al., 2014) the lake has now expanded to a range (926 m lake surface elevation above sea level) that have not been observed in the last 10 years. The rising lake level is marked by drowned trees and vegetation which are now decomposing along the flooded margin and floor of Lake Ngami (Fig. 1). The decomposition of tress and grasses within the lake is expected to affect the dissolved organic carbon (DOC) in the water column and lake sediments as well as the lake's carbon balance.

CHAPTER III

METHODOLOGY

Section 1. Sample Collection

Inflow into Lake Ngami occurs from the Kunyere River distributary and the Nhabe River (Fig. 1). The Nhabe River flows to the southeast where it joins the Kunyere River to flow into Lake Ngami approximately 12 km from the inlet. Samples were collected by boat from 19 stations at about 1.0 km spacing along an 18.1 km axial transect of Lake Ngami during peak flooding in the lower Okavango Delta in July 2012. The survey commenced in the river inlet 0.5 km above the mouth and continued to the distal edge of the lake, passing through the center of the lake. All locations along the transect where drowned vegetation along the edges of the lake transitioned to open water were noted (Fig. 1).

At each station, we collected water samples at a depth of 25 cm using a 2.2 L Van Dorn Beta Horizontal Acrylic Water Sampler (Wildlife Supply Company). The samples were filtered through 0.45 µm nylon syringe filters after collection. Samples for anions were stored un-acidified in 30 mL HDPE bottles and samples for cations were stored in 60 mL HDPE bottles that were pre-acidified with high purity nitric acid to a pH < 2.

Samples used to determine the dissolved inorganic carbon (DIC) concentration and the stable carbon isotope ratio of DIC ($\delta^{13}C_{DIC}$) were collected in 15 mL pre-evacuated vacutainer tubes pre-loaded with 1 mL of 85% H_3PO_4 and magnetic stir bars (Atekwana and Krishnamurthy, 1998). Water samples for stable isotopes of hydrogen (δD) and oxygen ($\delta^{18}O$) analysis were collected in 20 ml scintillation vials with inverted cone closures. Samples for the analysis of stable carbon isotope ratio of particulate organic carbon ($\delta^{13}C_{POC}$) were collected by filtering 1 L of lake water through a pre-combusted GF/F glass microfiber filter (Whatman cat. No. 1825-047). The filters were folded and stored in pre-combusted aluminum foil until analysis. After collection, all samples were protected from sunlight and stored under cool conditions. Samples were kept in a portable 12 V refrigerated cooler for 2 weeks before transportation to the United States where they were stored in a refrigerator at 4 °C until analysis.

Section 2. Measurements and Sample Analysis

At each sampling station, we measured water depth using a weighted graduated rope and water clarity using a secchi disc. At each sampling location, water temperature, pH, dissolved oxygen (DO), total dissolved solids (TDS) and specific conductance were measured in situ with a Yellow Springs Instrument multi-parameter probe (YSI 556MPS) calibrated according to the manufacturer's recommendations. After filtration in the field, aliquots of the water samples were immediately titrated for total alkalinity with sulfuric acid (Hach Company, 1992). In the laboratory, anions and cations were analyzed by ion chromatography using a Dionex ICS-3000 (Dionex, Sunnyvale, CA). Samples were

introduced to the ion chromatograph with a 50 µL sample loop to increase detection sensitivity. All samples were within our calibration range, with the lower end at 0.01 mg/L. The samples were each measured in triplicate and these results were averaged. The replicates agreed within 5% and repeated measurements of calibration standards were in agreement better than 3%. Samples for DOC and total nitrogen (TN) content were determined using a Shimadzu TOC-V Total Organic Carbon/Total Nitrogen 206 Analyzer with high salts kit, which includes components designed to reduce clogging of the catalyst in samples with high salt concentrations. Samples were acidified with HCl and sparged for 5 minutes with high purity N_2 gas to remove inorganic carbon. The δD and δ^{18}O were determine by high temperature conversion elemental analyzer (TC/EA) (Gehre et al., 2004) coupled to a Finnigan Delta Plus XL isotope ratio mass spectrometer. Filters containing POC samples were acidified by fumigating in a plastic bin using 100 mL of concentrated HCl place in a beaker. The acidified filters were dried for 24 hours at 60 ºC. A portion of the filter was cut and combusted in quartz tubes (Boutton et al., 1983). The $CO_{2(g)}$ was then purified on a vacuum line and sealed in Pyrex tubes. $\delta^{13}C_{POC}$ was measured from the extracted $CO_{2(g)}$ with a Thermo Finnigan Delta Plus XL isotope ratio mass spectrometer. For DIC analysis, $CO_{2(g)}$ was extracted from the vacutainer tubes under vacuum and the $CO_{2(g)}$ concentrations were determined empirically (Atekwana and Krishnamurthy, 1998). The extracted $CO_{2(g)}$ was sealed in pyrex tubes and later measured for stable carbon isotopes using a Thermo Finnigan Delta Plus XL isotope ratio mass spectrometer. The stable isotope ratios are reported in the delta notation (δ) in per mil (‰):

$$\delta\ (‰) = [(R_{sample} - R_{standard}) / R_{standard}]*1000$$

Where R is $^{18}O/^{16}O$ or $^{13}C/^{12}C$. The δ values are reported relative to VSMOW standard for $\delta^{18}O$ and δD and relative to VPDB standard for $\delta^{13}C$. Routine measurements of in-house standards and replicate samples have an overall precision of better than 2.0‰ for δD, 0.2‰ for $\delta^{18}O$ and 0.1‰ for $\delta^{13}C$.

CHAPTER IV

FINDINGS

Section 1. Water Depth, Secci Depth, Temperature and Dissolved Oxygen

The results of the water depth, secci depth, temperature and DO concentrations are presented in Table 1. Plots of water depth, secci depth, temperature and DO concentrations along the transect are shown in Figure 2. Water depth varied between 0.5 and 3.9 m and increased from 0.5 to 3.8 m from station 1 to 6.3 km, remained between 3.3 and 3.9 m from 6.3 km until 15.7 km and then began to shallow at 16.5 km to the end of the transect, to a depth of 2.0 m(Fig. 2a). Light penetration measured by the secci disc ranged from 0.6 to 0.9 m. The secci depth was shallower between 0.75 and 0.70 m from station 1 to 4.2 km, increased from 0.85 to 0.90 m to 8.3 km, remained between 0.75 and 0.80 m to 16.5 km and then decreased to 0.6 m to 18.1 km (Fig. 2b). Water temperature ranged from 13.5 to 16.8° C. Excluding station 1, before the river mouth, the temperature varied between 13.5 and 14.7 °C across the lake (Fig. 2c). DO ranged from 6.76 to 9.82 mg/L and showed an overall increasing trend along the transect (Fig. 2d).

Section 2. TDS, $\delta^{18}O$, Na^+, and Ca^{2+}

The results of TDS, $\delta^{18}O$, Na^+, and Ca^{2+} are presented in Table 1 and plots of variations in these parameters are presented in Figure 2. The TDS ranged from 75 to 141 mg/L. TDS from station 1 to 5.3 km ranged from 75 to 80 mg/L which increased to 120 mg/L to 10.2 km, and remained between 111 and 119 mg/L to 13.1 km before increasing continuously to 140 mg/L to the end of the transect at 18.1 km (Fig. 2e). A characteristic segmentation into three regions from the inlet river at station 1 to 5.3 km, from 5.3 to 13.1 km and from 13.1 to 18.1 km is observed in the TDS concentrations along the transect. The $\delta^{18}O$ ranged from 1.3‰ to 7.5‰ and the δD from 0.9‰ to 26.5‰. The axial enrichments of the $\delta^{18}O$ (Fig. 2f) and δD (Table 1) along the profile show spatial variations similar to the TDS results (Fig. 2e); their isotopic variations are lower from station 1 to 5.3 km, increase from 5.3 to 13.1 km and then increase further to 18.1 km. Concentrations of Na^+ ranged from 9.0 to 14.8 mg/L, and Ca^{2+} ranged from 9.8 to 20.6 mg/L. The concentrations of Na^+ (Fig. 2g), Mg^{2+} (Table 1) and Ca^{2+} (Fig. 2h) show spatial variations similar to variations in TDS concentrations (Fig. 2e) and the $\delta^{18}O$ (Fig. 2f); their concentrations are low from station one to 5.3 km, then increase from 5.3 km to 13.1 km and increase even further from 13.1 km to 18.1 km.

Section 3. Cl^-, SO_4^{2-}, NO_3^- and NH_4^+

The concentrations of Cl^-, SO_4^{2-}, NO_3^- and NH_4^+ are presented in Table 1 and displayed graphically in Figure 3. The concentrations of Cl^- ranged from 1.0 to 2.6 mg/L. The axial variations of Cl^- (Fig. 3a) across the transect show spatial variations similar to TDS, $\delta^{18}O$, Na^+ and Ca^{2+} concentrations (Fig. 2e-h). The concentrations of SO_4^{2-} ranged

from 0.07 to 0.14 mg/L and NO_3^- from non-detectable (<0.01 mg/L) to 0.38 mg/L. Overall, the SO_4^{2-} concentrations increase from station 1 to the maximum value of 0.14 mg/L at 8.2 km before decreasing at 11.2 km to 0.06 mg/L at the end of the transect (Fig. 3b). The variations in SO_4^{2-} are such that the concentrations are symmetrical about the center of the lake, with peak concentrations occurring near the middle and lower concentrations near the edges of the lake. The NO_3^- concentrations, although variable, show relatively increasing concentrations away from the edges of the lake and decrease near the middle (9.1 to 14.9 km) of the lake (Fig. 3c). In fact, the NO_3^- concentration at 14 km near the middle of the lake was below the instrument detection limit. Concentrations of NH_4^+ show an overall trend similar to NO_3^- and increase from station 1 to a maximum of 0.42 mg/L at 7.1 km. The NH_4^+ concentrations then decrease in the center of the lake before increasing at the end of the transect (Fig 3d).

Section 4. pH, HCO_3^-, DIC and $\delta^{13}C_{DIC}$

The results of the pH, HCO_3^- and DIC concentrations and the $\delta^{13}C_{DIC}$ are presented in Table 1. The pH of the lake water ranged from 6.98 to 8.07. The pH is nearly constant from station 1 to 6.3 km, then increases steadily until 11.2 km, and decreases towards 14.9 km before increasing again to the end of the transect (Fig. 3e). The concentrations of HCO_3^- ranged from 62.0 to 130.0 mg/L. The axial variations in HCO_3^- (Fig. 3f) are similar to that of TDS, $\delta^{13}O$, Na^+ and Ca^{2+} concentrations (Fig. 2e-h). The DIC concentrations ranged from 9.9 to 19.1 mg C/L and $\delta^{13}C_{DIC}$ ranged from -8.2 to 0.2 ‰ (Table 1) The DIC concentrations (Fig. 3g) and $\delta^{13}C_{DIC}$ (Fig. 3h) increase along

the transect and reach a nearly steady state beyond 8.25 km for DIC concentrations and 11 km for $\delta^{13}C_{DIC}$.

Section 5. DOC, TN, and $\delta^{13}C_{POC}$

Results for DOC, TN and $\delta^{13}C_{POC}$ measurements made at four points along the transect including station 1 at the inlet river, are presented in Table 1. DOC ranged from 15.36 to 24.89 mg/L and TN concentrations ranged from 1.91 to 3.09 mg/L. Axial variations of the DOC and TN concentrations mirror each other; both are low at station 1 and 6.3 km into the lake. Their concentrations are highest in the center of the lake where they remain high to the end of the lake transect, similar to the DIC concentrations (Fig. 3g). The $\delta^{13}C_{POC}$ ranged from -24.2‰ to -29.1‰, with the heaviest value (-24.2‰) observed at station 1 in the river inlet (Table 1). The $\delta^{13}C_{POC}$ within the lake is significantly more negative (-27.1‰ to -29.1‰) than that of the inflow water.

CHAPTER V

DISCUSSION

Section 1. Influence of Internal Chemical Processes

The survey of the major ion chemistry and the stable isotopes of hydrogen, oxygen and carbon of Lake Ngami show that (1) the water chemistry and stable isotopes are significantly different from that of the source rivers, (2) moving through the lake, there is increase in TDS (Fig. 2e), the $\delta^{18}O$ and the concentrations of Na^{+}, Ca^{2+} (Fig 2e-h), Cl^{-} (Fig. 3a) and HCO_3^{-} (Fig. 3f), all of which show a three tiered segmentation along the longitudinal axis of the lake, (3) there is an axial increase in the concentrations of SO_4^{2-} towards the center of the lake and a decrease toward the lake margins (Fig. 3b), whereas, the concentrations of NO_3^{-} (Fig. 3c) show an overall increase from the inlet and decrease around the center of the lake; and (4) overall, pH (Fig. 3e), DIC (Fig. 3g), and $\delta^{13}C_{DIC}$ (Fig. 3h), are relatively constant near the river mouth and lake inlet and then increase dramatically around the center of the lake. These parameters then decrease slightly before increasing to the distal portion of the lake. The results of the chemical and isotopic properties suggest that river water discharged into the lake undergoes further physical, chemical and isotopic evolution. Also, the pH as well as concentrations of SO_4^{2-}, NO_3^{-}, DIC, and the $\delta^{13}C_{DIC}$,

exhibit longitudinal behavior that differs from the TDS, $\delta^{18}O$, Na^+ and Ca^{2+} (Fig. 2e-h). Consequently, we can infer that the cycling of SO_4^{2-}, NO_3^-, and C occurs internally within the lake. To understand the changes in the lake water chemical properties, we elucidate the processes responsible for increases in the concentrations of the major ions, as well as those that affect the production and consumption of SO_4^{2-}, NO_3^- and C.

Section 2. Enrichment of Solutes in Lake Ngami

Lake Ngami receives inflow exclusively from surface water (the Kunyere and Nhabe Rivers). Groundwater table elevations are below lake bed elevation depicted in the groundwater level contour map of the Okavango Delta (McCarthy and Bloem, 1998). This eliminates recharge from groundwater, which has much higher solute concentrations (McCarthy and McIver, 1991; Linn et al., 2002; Ramberg and Wolski, 2008). Consequently, the enrichment of solutes in the Lake Ngami can arise from either the dissolution of salts that were precipitated on the lake bed during the previous desiccation cycle of the lake or from evaporative concentration, both of which occur elsewhere in this semi-arid region. There is no data on the soluble salts of the dry lake bed sediments of Lake Ngami, and therefore we are unable to conclusively assess the role of salt dissolution from the lake bed. A Google Earth™ image taken in 2006 does not show salt precipitates in the dry lake bed as is characteristic of several of the pans in the region and islands in the Okavango Delta. Nevertheless, if the increase of solutes in the lake water was solely attributed to the dissolution of salts from the lake bed and sediments, then the longitudinal profiles of solute concentrations in the lake would be expected to be more

uniform and not segmented in such a way that suggests multiple controls on the major ionic concentrations.

To assess the role of evaporative enrichment, we examine the relationship between $\delta^{18}O$ and δD in Lake Ngami (Fig. 4a). The $\delta^{18}O$ and δD plot along a line with a least squares regression equation of: $\delta D = 4.7\ \delta^{18}O - 8.6$ ($r^2 = 0.98$), which is similar to the evaporative water line for surface water in the Okavango Delta region (Mazor et al., 1977; Dincer et al., 1979; Linn et al., 2002; Akoko et al., 2013). This line is shown in Figure 4b. If evaporation is responsible for the increase in the concentration of the solutes, then the change in the solutes concentrations represented by the TDS, for example, should be related to the $\delta^{18}O$ and δD (e.g., Simpson and Herczeg, 1991; Huang and Pang, 2012). The relationship between TDS and $\delta^{18}O$ for Lake Ngami is defined by the logarithmic regression equation: $\delta^{18}O = 7.6[(\ln)TDS] - 30.5$, with a good correlation coefficient (r^2) of 0.93 (Fig. 4c). This suggest that the increases in solute concentrations in the lake can be attributed to evaporative concentration, which is consistent with the effects of evapotranspiration concentration of solutes in surface water observed in the Okavango Delta (Dincer et al., 1979; Sawula and Martins, 1991; Cronberg et al., 1995; Krah et al., 2006; Bauer-Gottwein et al., 2007; Ramberg and Wolski, 2008; Mackay et al., 2011; Mmualefe and Torto, 2011; Akoko et al., 2013).

Although the role of transpiration was not assessed, it is unlikely to be significant. Most of the terrestrial vegetation in the lake, especially trees, are dead, and spatial distribution of emergent aquatic vegetation as well as its overall density in the lake is significantly lower than in the Okavango River and its distributaries. We estimate from visual inspection, that less than 5% of the lake is covered by emergent aquatic

vegetation (Fig. 1). Moreover, the uptake of water by plants is non-fractionating with respect to the $\delta^{18}O$ and δD (e.g., Walker and Richardson, 1991). The sparse distribution of vegetation could account for the lack of scatter observed in the TDS vs. $\delta^{18}O$ relationship shown in Figure 4c.

Input of water into Lake Ngami consists exclusively of discharge from the Kunyere and Nhabe Rivers. The TDS and major cations concentrations of both rivers from the floods of 2010, 2011, and 2012 (Table 1) are relatively consistent from year to year. For example, the TDS concentrations from the three years for the Nhabe River (76 $\pm$ 2 mg/L) and Kunyere River (83 $\pm$ 5.1 mg/L) deviate by less than 7%. This fact suggests that the segmented increases in both TDS and the major cations in Lake Ngami are not due to chemical variations of inflow. To explain the segmentation of the solute enrichment axially across Lake Ngami, we suggest differential enrichment by evaporation. This differential enrichment is due to the fact that water delivery into Lake Ngami occurs mainly from the annual flood pulses that supply water to the Okavango Delta from March through September (e.g., Mackay et al., 2011). Local rains which occur from November to February (McCarthy and Bloem, 1998) are expected to contribute little to the lake water compared to annual flooding. The amount of rainfall contributed to surface water in the region is currently unknown. However, inspection of average monthly discharge hydrographs in Maun demonstrate no significant increase due to seasonal rains (Gieske, 1997). Limited local precipitation during the rainy season is likely to contribute to the seasonally low water table (Milzow et al., 2009). Isotopically lighter rainwater has been shown to be the main constituent of groundwater in this region (Dincer et al., 1979). Therefore, we assume in the absence of additional data that there is

negligible contribution from local meteoric water to Lake Ngami and that precipitation is likely to have a small effect on the lake volume and chemical composition. Since Lake Ngami has no outlet, our assumption is valid; changes in the lake water properties persist for almost a year before recharge occurs from fresh influx from annual flooding of the Okavango Delta.

It can be safely argued that the segmentation in the solute concentrations which increase axially from the proximal to the distal portion of the lake is due to the extent of physical and chemical changes in the lake. Due to a lack of outflow from the lake, the water is trapped and undergoes physical and chemical transformation before the next flood recharge. The first segment on the plots of TDS and cations (roughly 0-5 km into the lake (e.g., Fig. 2e,g,h) denotes the most recent inflow (2012) and is characterized by the lowest solute concentrations. The farthest segment along the transect (roughly 13 km to the distal portion of the lake) is interpreted as the inflow contributions from the 2010 flood. The cause for such distinction in the chemical composition is directly related to varying residence time, resulting in differential exposure of lake water to evaporative effects. This has the greatest effect on the oldest recharge. In this scenario, the oldest recharge (2010) is located in the distal portion of the lake, and the effects of dilution from subsequent annual recharge increase toward the river inlet. Therefore, the three segmentations in the chemical data suggest slow lateral mixing and homogenization in Lake Ngami during the initial stages of filling.

Section 3. Carbon and Nutrient Cycling in Lake Ngami

In Lake Ngami, the DIC concentrations (Fig. 3g) and $\delta^{13}C_{DIC}$ (Fig. 3h) vary longitudinally across the lake. The longitudinal trends in both parameters are characterized by relatively low values in the proximal end of the lake, which sharply increase to the center before leveling off in the distal portion of the lake. The DIC concentrations and $\delta^{13}C_{DIC}$ are correlated ($r^2 = 0.8$) and even though the data are distributed in two main clusters (Fig. 5a), they are consistent with the longitudinal variations (Fig. 3g and h). The processes that potentially influence carbon cycling within Lake Ngami are (1) evaporative enrichment of the concentration of DIC, (2) microbial breakdown of organic matter (OM) in the water column and lake bed sediments, (3) water column photosynthesis and photo-oxidation of OM and (4) carbon loss and or/exchange between DIC and atmospheric $CO_{2(g)}$.

Evapoconcentration of solutes has been documented in surface water of the Okavango Delta (Dincer et al., 1979; Sawula and Martins, 1991; Krah et al., 2006; Bauer-Gottwein et al., 2007; Ramberg and Wolski, 2008; Mackay et al., 2011; Mmualefe and Torto, 2011; Akoko et al., 2013). Results of this work favor evapoconcentration of solutes in lake Ngami considering the relationship between TDS and $\delta^{18}O$ (Fig. 4c) in the previous section. To demonstrate the extent to which evapoconcentration affects the DIC concentrations, we plot the TDS concentrations vs. DIC concentrations (Fig. 5b). A least squares regression through the data (DIC = 7.21TDS +10.9) has a good correlation coefficient (r^2=0.82). Again, as in the case of DIC vs. $\delta^{13}C_{DIC}$, the data are clustered into two groups. We suggest that although evapoconcentration is directly related to the increase in major ion concentrations, it is only partially responsible for the increase in

DIC concentrations in the lake. We make this distinction because if the DIC variations in the lake were solely related to evapoconcentration, the $\delta^{13}C_{DIC}$ would be expected to remain constant. In order to elucidate the role of evapotranspiration on the $\delta^{13}C_{DIC}$ values, we use $\delta^{18}O$ as a proxy for evapoconcentration and plot the $\delta^{13}C_{DIC}$ vs. $\delta^{18}O$ (Fig. 5c). A least squares regression through the data ($\delta^{18}O = 0.56\delta^{13}C_{DIC} + 6.6$) has a good correlation (r^2=0.92). Although there is good relationship between DIC and TDS, we suggest that this is coincidental, and is mainly due to the fact that the extent of evaporation is time dependent and time dependence may also affect the extent of isotopic enrichment of the $\delta^{13}C_{DIC}$.

The overall increase in $\delta^{13}C_{DIC}$ in the lake water indicates that processes that increase the $\delta^{13}C_{DIC}$ dominate over those that cause a decrease in the $\delta^{13}C_{DIC}$. Processes that cause a decrease in the $\delta^{13}C_{DIC}$ such as respiration (e.g., Quay et al., 1986; Wachniew and Rozanski, 1997) or photo-oxidation of organic matter in the water column (e.g., Mopper et al., 1991) have less dominance over processes that increase the $\delta^{13}C_{DIC}$, such as photosynthesis (e.g., Farquhar et al., 1989) and carbon equilibration between DIC and atmospheric $CO_{2(g)}$. Respiration and photo-oxidation produce $CO_{2(g)}$ with a $\delta^{13}C$ composition of that of the organic matter being processed. A study of stable carbon isotopes of successional vegetation in a distributary of the Okavango River shows that material is supplied primarily by deep water submerged, floating-leaved, and tall emergent vegetation species, which contribute $\delta^{13}C$ between -26 and -27‰ (Ellery et al., 1992). Mladenov et al. (2007) report the $\delta^{13}C$ for the giant C4 sedge *Cyperus papyrus* which commonly lines channels of -11.6‰, the common wetland C4 grass *Panicum repens* of -12.2‰ and the C3 grass *Oryza longistaminata* of -25.3‰. Despite the

possibility of both C4 and C3 vegetation contributing to organic matter in the river channels, the $\delta^{13}C$ for DOC across the Okavango Delta averages -25.6 $\pm$ 1.6‰ during the non-flood season and -24.9 $\pm$ 1.3‰ during flood season (Akoko et al., 2013), suggesting the dominance of C_3 vegetation contribution to the riverine DOC pool. This DOC is transported to Lake Nagmi by the Kunyere and Nhabe Rivers. The $\delta^{13}C_{POC}$ measured in the lake ranged from -27.1‰ to -29.1‰, thus, contribution of $CO_{2(g)}$ from respiration and photo-oxidation of OM to the lake DIC pool should increase the pCO_2 and DIC concentrations and decrease the $\delta^{13}C$ of DIC. A plot of the log pCO_2 along the sampled transect shows a continuous overall decrease (Fig. 6a), even though the DIC concentrations generally increase along the transect (Fig. 3g). The overall decrease in log pCO_2 along the transect and the increasing $\delta^{13}C$ of DIC indicates that $CO_{2(g)}$ generated from organic matter respiration or photo-oxidation of organic matter is relatively small and that the lake water is experiencing $CO_{2(g)}$ loss. Loss of $CO_{2(g)}$ to the atmosphere or uptake by photosynthesis results in an increase in pH. Thus, the general increase in the pH along the transect (Fig. 3e) is consistent with $CO_{2(g)}$ removal from the DIC pool as a function of distance along the transect. Again, this distance is analogous with residence time of water in the lake.

Both photosynthesis and loss of $CO_{2(g)}$ from aquatic DIC will enrich ^{13}C of DIC. To distinguish which of the processes is primarily responsible for the shift in the $\delta^{13}C_{DIC}$, we plot the pCO_2 vs. $\delta^{13}C_{DIC}$ (Fig. 6b). The data shows that as pCO_2 is decreasing, the $\delta^{13}C_{DIC}$ is increasing (depicted by arrow 1). This trend appears to reach quasi-equilibrium at a $\delta^{13}C_{DIC}$ value of -1.0 $\pm$ 0.6‰ depicted by arrow 2. The equilibrium fractionation for the transformation of HCO_3^- to $CO_{2(g)}$ is about 9‰ (e.g., Mook, 1974)

for lake water temperature averaging 14 $\pm$ 0.4 ºC and an assumed $\delta^{13}C$ of atmospheric $CO_{2(g)}$ of -8‰ (Allison et al., 2003). Because we measured the water temperature in winter during a single day, our data may not represent the range in temperature that is responsible for the isotopic fraction during equilibration with atmospheric $CO_{2(g)}$. Nevertheless, the results suggest that equilibration of aquatic DIC with atmospheric $CO_{2(g)}$ is likely dominant over aquatic photosynthesis.

Similar to the Okavango River and distributaries, nutrient levels and primary productivity are assumed to be low in the lake (Sawula and Martins, 1991; Cronberg et al., 1995; Krah et al., 2006). Although not significant in the lake's overall isotopic record, there is a slight decrease in the $\delta^{13}C_{DIC}$ between 10 and 15 km along the lake transect (Fig. 3h). In the same distance region, there are also noticeable decreases in DIC concentrations (Fig. 3g), pH (Fig. 3e), NO_3^- (Fig. 3c) and NH_4^+ (Fig. 3d). The concentration variability of SO_4^{2-} and NO_3^- along the lake transect are small; 0.06 to 0.14 mg/L for SO_4^{2-} and below detection to 0.39 mg/L for NO_3^-. However, these parameters can indicate the coupling of nitrogen and sulfur cycling to that of carbon. Because of the low nutrient availability in the lake, OM in the water column can be mineralized by microbes through respiration (Cronberg et al., 1995) and photo-oxidation (Mladenov et al., 2005). There are higher DOC and TN concentrations (Table 1) near the middle of the lake which we suggest is linked to the increased microbial processing of OM in this region. Oxidation of OM can generates HS^- which is utilized by sulfur oxidizing bacteria (SOB). The SOB reduces NO_3^-, resulting in loss of N_2 through denitrification and production of elemental sulfur which may be further oxidized to SO_4^{2-} (Fossing et al., 1995).

$$2NO_3^- + 5HS^- + 7H^+ \rightarrow N_2 + 5S + 6H_2O \quad (1)$$

$$6NO_3^- + 5S + 2H_2O \rightarrow 3N_2 + 5SO_4^{2-} + 4H^+ \quad (2)$$

Bacterial utilization of NO_3^- in conjunction with S-cycling has been observed in freshwater (Burgin and Hamilton, 2008) and we hypothesize that this is the main process contributing to elevated levels of SO_4^{2-} that are coupled with denitrification in the lake's center. This consumption of inorganic nitrogen is evident by the clear decrease in percent inorganic nitrogen (Table 1) within the center of the lake (measured at 11.2 and 14.0 km). The slight decrease in $\delta^{13}C_{DIC}$ for this same region is also indicative of the oxidative degradation of OM, as the $\delta^{13}C_{DIC}$ values shift to slightly more negative values (Fig. 3g). We also observed that the overall axial decrease in the pCO_2 stops at 10 km where it increases to 15 km before decreasing (Fig. 6b). The increase in the pCO_2 is likely due to production of $CO_{2(g)}$ in the water column. We suggest that the $\delta^{13}C_{DIC}$ value of -1.0 $\pm$ 0.6‰ for lake water at 10 to 15 km is the quasi equilibrium state controlled by the balance between carbon isotopic equilibration between aquatic DIC and atmospheric $CO_{2(g)}$ and water column production $CO_{2(g)}$ from the respiration and photo-oxidation of organic matter.

CHAPTER VI

CONCLUSIONS

In this study, we measured physical parameters as well as chemical and stable isotope composition of water along an axial transect of a filling lake in a semi-arid region. Our results show that the increase in concentration of solutes was not linear across the lake but instead segmented into three regions, explained by the punctuated annual recharge which subjects each season's inflow to differential evaporation during periods of no significant inflow. Our findings demonstrate that water within the lake is affected by evapoconcentration of solutes as well as carbon and nutrient cycling. Solutes (e.g., Cl^-, Na^+, Mg^{2+}, Ca^{2+}) increase in concentration from the river mouth to the distal portion of the lake. This increase in concentration is attributed to evapoconcentration, which is made evident by the concomitant enrichment of TDS and $\delta^{18}O$ typical of semiarid regions.

Evapoconcentration in Lake Ngami is also partially responsible for the longitudinal increase in DIC concentration, although a longitudinal variation in $\delta^{13}C_{DIC}$ suggests that the evaporative effect is accompanied by other internal processes. Both DIC and $\delta^{13}C_{DIC}$ appear to reach equilibrium mid-way through the measured transect, at which point, the parameters attain nearly steady state. This equilibration is dictated by

the balance between evapoconcentration of DIC within the lake, DIC exchange with atmospheric $CO_{2(g)}$, and production of $CO_{2(g)}$ from water column respiration and perhaps photo-oxidation. A local increase in pCO_2 between 10 and 15 km of the transect indicates a linkage between carbon and nutrient cycling in response to microbial degradation. Finally, we conclude that the three segments exhibited in the chemical data suggest slow lateral mixing and homogenization in Lake Ngami during the initial stages of filling.

CHAPTER VII

FUTURE WORK

The conclusions drawn from this study are the result of a single longitudinal survey, conducted during one day of the winter flood season in the Okavango Delta. In order to continue research of chemical cycling in Lake Ngami, more work should be conducted to supplement these conclusions. The most fundamental future contribution could be carried out by continued monitoring, both annually and seasonally. Not only would this information be beneficial to the observation of lake levels in response to varying seasonal inflow, but annual studies following a similar transect could provide information on the longitudinal stratification of the major solute species and provide insight on the status of chemical homogenization within the lake. In addition to continued annual sampling, future studies could also examine the chemical properties in Lake Ngami throughout multiple seasons, in order to analyze temporal effects. Seasonal studies would be especially beneficial to the interpretation of nutrient and carbon cycling, as influx of organic material into the lake would be expected to be seasonally variable.

The manner of the measured survey could also be altered to provide more information about chemical cycling within Lake Ngami. This survey investigated the top 25 cm of the water column along a longitudinal transect to assess the overall lake chemistry. Investigating samples from multiple depths for isotopic and chemical variations can confirm our assertion based on multiple YSI readings, that the water column is indeed mixed. A transect measured though transverse section of the lake may also be beneficial to future work as solute concentrations would theoretically remain relatively consistent along a chosen transverse section, however nutrient and carbon concentrations are expected to change as the survey proceeds from the vegetated margin of the lake, through the open center, and into the vegetated margin along the opposite shoreline. This information can supplement our understanding of the cycling of carbon and nutrients within the lake.

To address other limitations of this study, the degradation of organic material in reference to S and N species should be investigated. This could be carried out by incubation experiments of lake bed sediments. By observing organic matter decay and relative concentrations of NO_3^- and SO_4^{2-} in the lake sediments, it would be possible to better conceptualize the nutrient/carbon cycling processes that were described in this study exclusively with water column data.

REFERENCES

Akoko, E., Atekwana, E.A., Cruse, A.M., Molwalefhe, L., Masamba, W.R.L., 2013. River-wetland interaction and carbon cycling in a semi-arid riverine system: the Okavango Delta, Botswana. Biogeochemistry 114, 359-380.

Allison, C.E., Francey, R.J., Krummel, P.B., 2003. Delta C-13 values (per mil) derived from CO_2 in flask air samples collected at Mawson, Antarctic. Atmospheric, Research, Commonwealth Scientific, and Industrial Research Organisation, Aspendale, Victoria, Australia 3195.

Andersson, L., Gumbricht, T., Hughes, D., Kniveton, D., Ringrose, S., Savenije, H., Todd, M., Wilk, J., Wolski, P., 2003. Water flow dynamics in the Okavango River Basin and Delta--a prerequisite for the ecosystems of the Delta. Physics and Chemistry of the Earth 28, 1165-1172.

Atekwana, E.A., Krishnamurthy, R.V., 1998. Seasonal variations of dissolved inorganic carbon and $\delta^{13}C$ of surface waters: Applications of a modified gas evolution technique. Journal of Hydrology 205, 265-278.

Bauer-Gottwein, P., Langer, T., Prommer, H., Wolski, P., Kinzelbach W., 2007. Okavango Delta Islands: Interaction between density-driven flow and geochemical reactions under evapo-concentration. Journal of Hydrology 335, 389-405.

Boutton, T.W., Wong, W.W., Hachey, D.L., Lee, L.S., Cabrera, M.P., Klein, P.D., 1983. Comparison of quartz and Pyrex tubes for combustion of organic samples for stable carbon isotope analysis. Analytical Chemistry 55, 1832-1833.

Bufford, K.M., Atekwana, E.A., Abdelsalam, M.G., Shemang, E., Atekwana, E.A., Mickus, K., Moidaki, M., Modisi, M.P., Molwalefhe, L., 2012. Geometry and faults tectonic activity of the Okavango Rift Zone, Botswana: Evidence from magnetotelluric and electrical resistivity tomography imaging. Journal of African Earth Sciences 65, 61-71.

Burgin, A.J., Hamilton, S.K., 2008. NO_3^-driven SO_4^{2-} production in freshwater ecosystems: Implications for N and S cycling. Ecosystems 11, 908-922.

Cronberg, G., Gieske, A., Martins, E., Prince Nengu, J., Stenstrom, I-M., 1995. Hydrobiolgical studies of the Okavango Delta and Kwando/Linyanti/Chobe River, Botswana .1. Surface water quality analysis. Botswana Notes and Records 27, 151-226.

Dincer, T., Hutton, L.G., Kupee B.B.J., 1979. Study, using stable isotopes, of flow distribution, surface-groundwater relations and evapotranspiration in the Okavango Swamp, Botswana. Isotope Hydrology 1, 3-26. IAEA (Int. Atomic Energy Agency), Vienna, Proc. Ser., SII/AUB/493 (1978).

Eckardt, F.D., Bryant, R.G., McCulloch, G., Spiro, B., Wood, W.W., 2008. The hydrochemistry of a semi-arid pan basin case study: Sau Pan, Makgadikagadi, Botswana. Applied Geochemistry 23, 1563-1580.

Ellery, K., Ellery, W.N., Verhagen, B.Th., 1992. The distribution of C_3 plant and C_4 plants in a successional sequence in the Okavango Delta. South African Journal of Botany 58, 400-402.

Farquhar, G.D., Ehleringer, J.R., Hubick, K.T., 1989. Carbon isotope discrimination and photosynthesis. Annual Review of Plant Physiology and Plant Molecular Biology 40, 503-537.

Fossing, H., Gallardo, V.A., Jorgensen, B.B., Huttel, M., Nielsen, L.P., Schulz, H., Canfield, D.E., Forster, S., Glud, R.N., Gundersen, J.K., Kuver, J., Ramsing, N.B., Teske, A., Thamdrup, B., Ulloa, O., 1995. Concentration and transport of nitrate by the mat-forming sulfur bacterium *Thioploca*. Nature 374, 713-715.

Gaughan, A.E., Waylen, P.R., 2012. Spatial and temporal precipitation variability in the Okavango-Kwando-Zambezi catchment, southern Africa. Journal of Arid Environments 82, 19-30.

Gehre, M., Geilmann, H., Richter, J., Werner, R.A., Brand, W.A., 2004. Continuous flow $^{2}H/^{1}H$ and $^{18}O/^{16}O$ analysis of water samples with dual inlet precision. Rapid Communication in Mass Spectrometry 18, 2650-2660.

Gieske, A., 1997. Modelling outflow from the Jao/Boro River system in the Okavango Delta, Botswana. Journal of Hydrology 193, 214-239.

Grove, A.T., 1969. Landforms and climatic change in the Kalahari and Ngamiland. Geographical Journal 135, 191-212.

Hach Company. 1992. Digital Titrator Model 16900-01 Manual. HACH Company, Loveland, Colorado.

Huang, T.M., Pang, Z.H., 2012. The role of deuterium excess in determining the water salinization mechanism: A case study of the arid Tarim River Basin, NW China. Applied Geochemistry 27, 2382-2388.

Huntsman-Mapila, P., Ringrose, S., Mackay, A.W., Downey, W.S., Modisi, M., Coetzee, S.H., Tiercelin, J.-J., Kampunzu, A.B., Vanderpost, C., 2006. Use of the geochemical and biogical sedimentary record in establishing palaeo-environments and climate change in the Lake Ngami basin, NW Botswana. Quaternary International 148, 51-64.

Kgathi, D.L., Kniveton, D., Ringrose, S., Turton, A.R., Vanderpost, C.H.M., Lundqvist, J., and Seely M., 2006. The Okavango; a river supporting its people, environment and economic development. Journal of Hydrology 331, 3-17.

Kinabo, B.D., Atekwana, E.A., Hogan, J.P., Modisi, M.P., Wheaton, D.D., Kampunzu, A.B., 2007. Early structural development of the Okavano rift zone, NW Botswana. Journal of African Earth Sciences 48, 125-136.

Kinabo, B.D., Hogan, J.P., Atekwana, E.A., Abdelsalam, M., Modisi, M.P., 2008. Fault growth and propagation during incipient continental rifting: Insights from a combined aeromagnetic and Shuttle Radar Topography Mission digital elevation model investigation of the Okavango Rift Zone, northwest Botswana. Tectonics 27, TC3013, doi: 10.1029/2007TC002154.

Krah, M., McCarthy, T.S., Huntsman-Mapila, P., Wolski, P., Annegarn, H., Sethebe, K., 2006. Nutrient budget in the seasonal wetland of the Okavango Delta, Botswana. Wetlands Ecology and Management 14, 253-267.

Laletsang, K., Modisi, M.P., Shemang, E.M., Moffat, L., Moagi, O.R., 2007. Shallow seismic refraction and magnetic studies at Lake Ngami, The Okavango Delta, Northwest Botswana. Journal of African Earth Sciences 48, 95-99.

Linn, F., Masie, M., Rana, A., 2002. The impacts on groundwater development on shallow aquifers in the lower Okavango Delta, northwestern Botswana. Environmental Geology 44, 112-118.

Mackay, A.W., Davidson, T., Wolski, P., Mazebedi, R., Masamba, W. R.L., Huntsman-Mapila, P., Todd, M., 2011. Spatial and seasonal variability in surface water chemistry in the Okavango Delta, Botswana: A multivariate approach. Wetlands 31, 815-829.

Mazor, E., Verhagen, B.Th., Sellschop, J.P.F., Robins, N.E., Hutton, L., Jennings, C.M.H., 1977. Northern Kalahari groundwaters: Hydrologic, isotopic and chemical studies at Orapa, Botswana. Journal of Hydrology 34, 203-234.

McCarthy, T.S., McIver, J.R., 1991. Groundwater evolution, chemical sedimentation and carbonate brine formation on an island in the Okavango Delta swamp, Botswana. Applied Geochemistry 6, 577-595.

McCarthy, T.S., Green, R.W., Franey, N.J., 1993. The influence of neo-tectonics on water dispersal in the northeastern regions of the Okavango swamps, Botswana. Journal of African Earth Sciences 17, 23-32.

McCarthy, T.S., Bloem, A., 1998. Observations on the hydrology and geohydrology of the Okavango Delta. South African Journal of Geology 101, 101-117.

McCarthy, T.S., Ellery, W.N., 1998. The Okavango Delta. Transactions of the Royal Society of South Africa 53, 157-182.

Milzow, C., Kgotlhang, L., Bauer-Gottwein, P., Meier, P., Kinzelbach, W., 2009. Regional review: the hydrology of the Okavango Delta, Botswana – processes, data and modeling. Hydrogeology Journal 17, 1297-1328.

Mladenov, N., McKnight, D.M., Wolski, P., Ramberg, L., 2005. Effects of annual flooding on dissolved organic carbon dynamics within a pristine wetland, the Okavango Delta, Botswana. Wetlands 25, 622-638.

Mladenov, N., McKnight, D.M., Wolski, P., Murray-Hudson, M. 2007. Simulation of DOM fluxes in a seasonal floodplain of the Okavango Delta, Botswana. Ecological Modeling 205, 181-195.

Mmualefe, L.C., Torto, N., 2011. Water quality in the Okavango Delta. Water SA 37, 411-418.

Modisi, M.P., 2000. Fault system at the southeastern boundary of the Okavango Rift, Botswana. Journal of African Earth Sciences 30, 569-578.

Mook, W.G., Bommerson, J.C., Staverman, W.H., 1974. Carbon isotope fractionation between dissolved bicarbonate and gaseous carbon dioxide. Earth and Planetary Science Letters 22, 169-176.

Mopper, K., Zhou, X., Kieber, R.J., Kieber, D.J., Sikorski, R.J., Jones, R.D., 1991. Photochemical degradation of dissolved organic carbon and its impact on the oceanic carbon cycle. Nature 353, 60-62.

Quay, P.D., Emerson, S. R., Quay, B.M., Devol, A.H., 1986. The carbon cycle for Lake Washington – A stable isotope study. Limnology and Oceanography 31, 596-611.

Ramberg, L., Wolski, P., 2008. Growing islands and sinking solutes: processes maintaining the endorheic Okavango Delta as a freshwater system. Plant Ecology 196, 215-231.

Ramberg, L., Wolski, P., Krah, M., 2006. Water balance and infiltration in a seasonal floodplain in the Okavango Delta, Botswana. Wetlands 26, 677-690.

Robbins, L.H., Murphy, M.L., Campbell, A.C., Brook, G.A., Reid, D.M., Haberyan, K.A., Downey, W.S., 1998. Test excavations and reconnaissance palaeoenvironmental work at Toteng, Botswana. South African Archaeological Bulletin 53, 125-132.

Robbins, L.H., Campbell, A.C., Murphy, M.L., Brook, G.A., Mabuse, A.A., Hitchcock, R.K., Babutsi, G., Mmolawa, M., Stewart, K.M., Steele, T.E., Klein, R.G., Appleton, C.C., 2009. Mogapelwa: Archaeology, palaeoenvironment and oral traditions at Lake Ngami, Botswana. South African Archaeological Bulletin 64, 13-32.

Sawula, G., Martins, E., 1991. Major ion chemistry of the lower Boro River, Okavango Delta, Botswana. Freshwater Biology 26, 481-493.

Shaw, P., 1985. The desiccation of Lake Ngami: An historical perspective. The Geographic Journal 151, 318-326.

Shaw, P., 1988. After the flood: The fluvio-lacustrine landforms of Northern Botswana. Earth-Science Reviews 25, 449-456.

Shaw, P.A., Bateman, M.D., Thomas, D.S.G., Davies, F., 2003. Holocene fluctuation of Lake Ngami, Middle Kalahari: chronology and responses to climatic change. Quaternary International 111, 23-35.

Simpson, H.J., Herczeg, A.L., 1991. Stable isotopes as an indicator of evaporation in the river Murry, Australia. Water Resources Research 27, 1925-1935.

Stigand, A.G., 1912. Notes on Ngamiland. Geographical Journal 39, 376-379.

Stigand, A.G., 1923. Ngamiland. Geographical Journal 62, 401-419.

Sutcliffe, J.V., Parks, Y.P., 1989. Comparative water balances of selected African wetlands. Hydrological Sciences 34, 49-62.

Wachniew, P., Rozanski, K., 1997. Carbon budget of mid-latitude, groundwater-controlled lake: Isotopic evidence for the importance of dissolved inorganic carbon recycling. Geochimica et Cosmochimica Acta 61, 2453-2465.

Walker, C.D., Richardson, S.B., 1991. The use of stable isotopes of water in characterizing the source of water in vegetation. Chemical Geology 94, 145-158.

Wolski, P., Murrary-Hudson, M., 2006. Recent changes in flooding in the Xudum distributary of the Okavango Delta and Lake Ngami, Botswana. South African Journal of Science 102, 173-176.

Wolski, P., Stone, D., Tadross, M., Wehner, M., Hewitson, B., 2014. Attribution of floods in the Okavango basin, Southern Africa. Journal of Hydrology 511, 350-358.

Zuber, A., 1983. On the environmental isotope method for determining the water balance components of some lakes. Journal of Hydrology 61, 409-427.

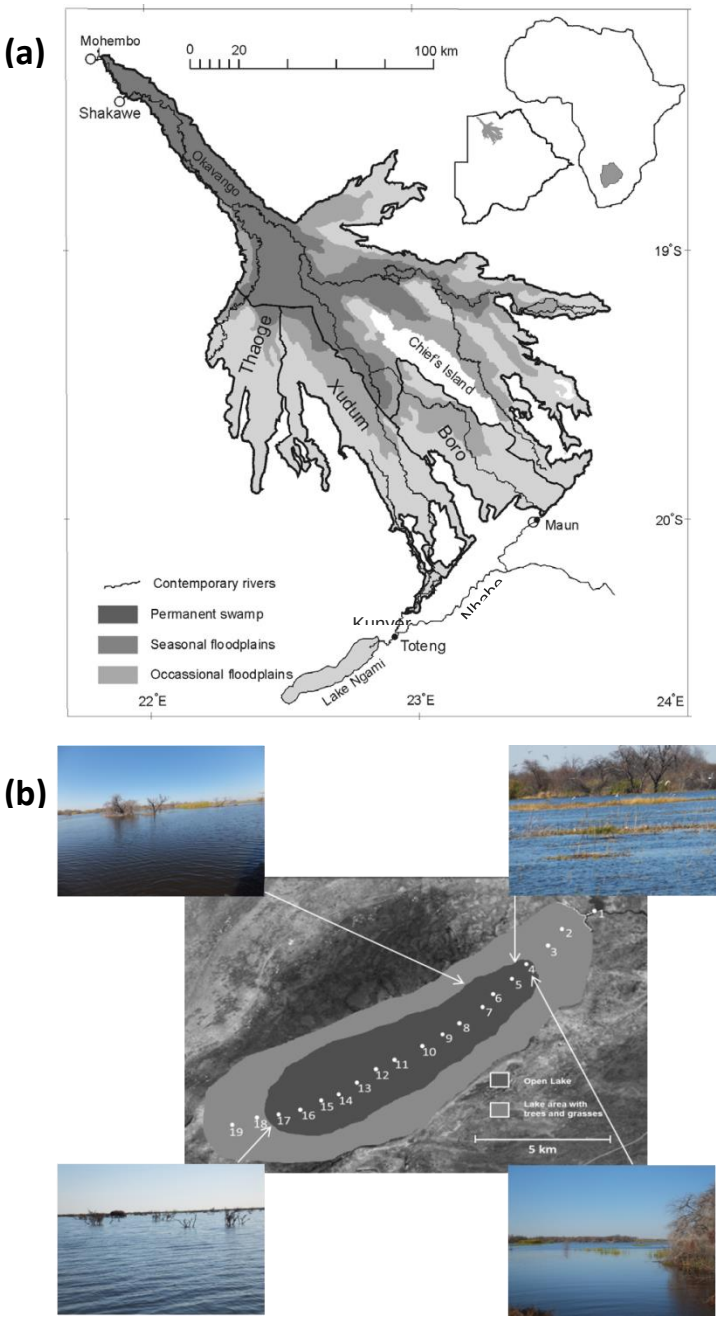

Fig. 1. (a) The Okavango Delta with distributary channels. Insert shows Africa and the locations of Botswana and The Okavango Delta. (Modified from Wolski and Murray-Hudson, 2006) and (b) Lake Ngami showing the outline of drowned vegetation and stations sampled across a longitudinal transect of the lake. Photographs show the nature of vegetation conditions at the edges of the lake from select locations.

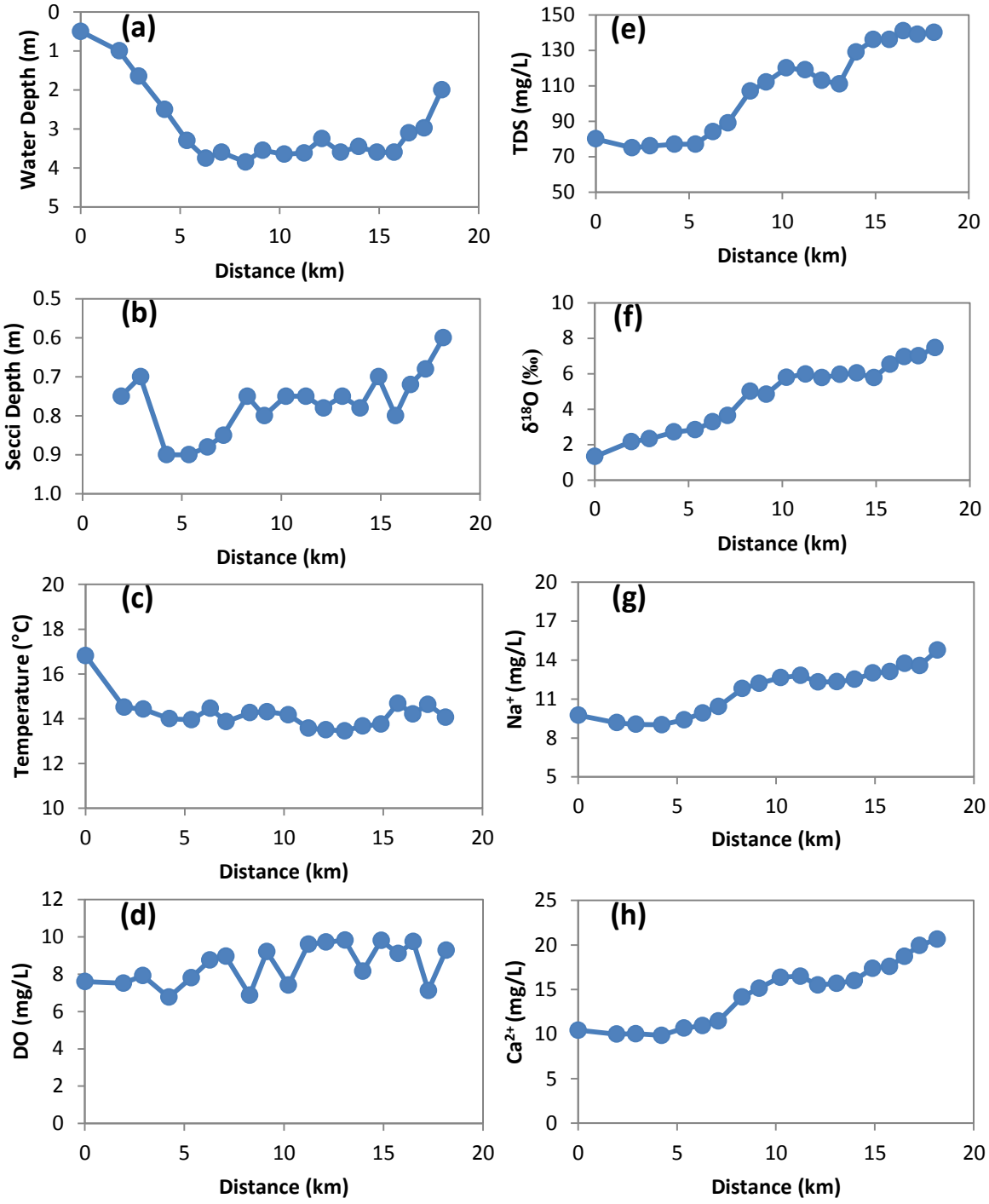

Fig. 2. (a) Axial plots of variations of water depth, (b) Secchi depth, (c) temperature and (d) dissolved oxygen (DO) concentrations and concentrations of (e) total dissolved solids (TDS), (f) $\delta^{18}O$, (g) Na^{+} and (h) Ca^{2+}.

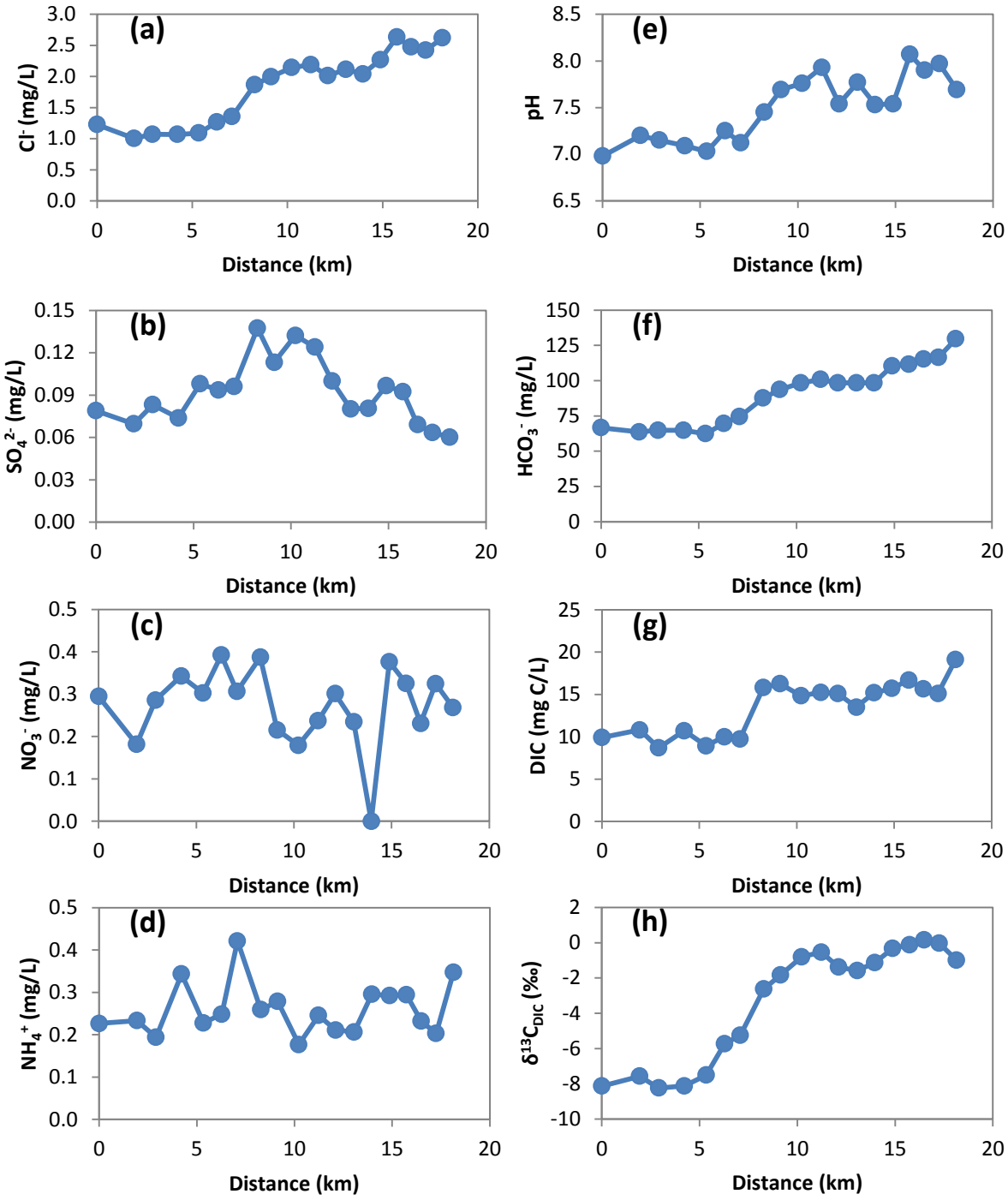

Fig. 3. Plot of axial variations of (a) Cl^-, (b) SO_4^{2-}, (c) NO_3^-, (d) NH_4^+, (e) pH, (f) HCO_3^-, (g) DIC, and (h) the $\delta^{13}C_{DIC}$.

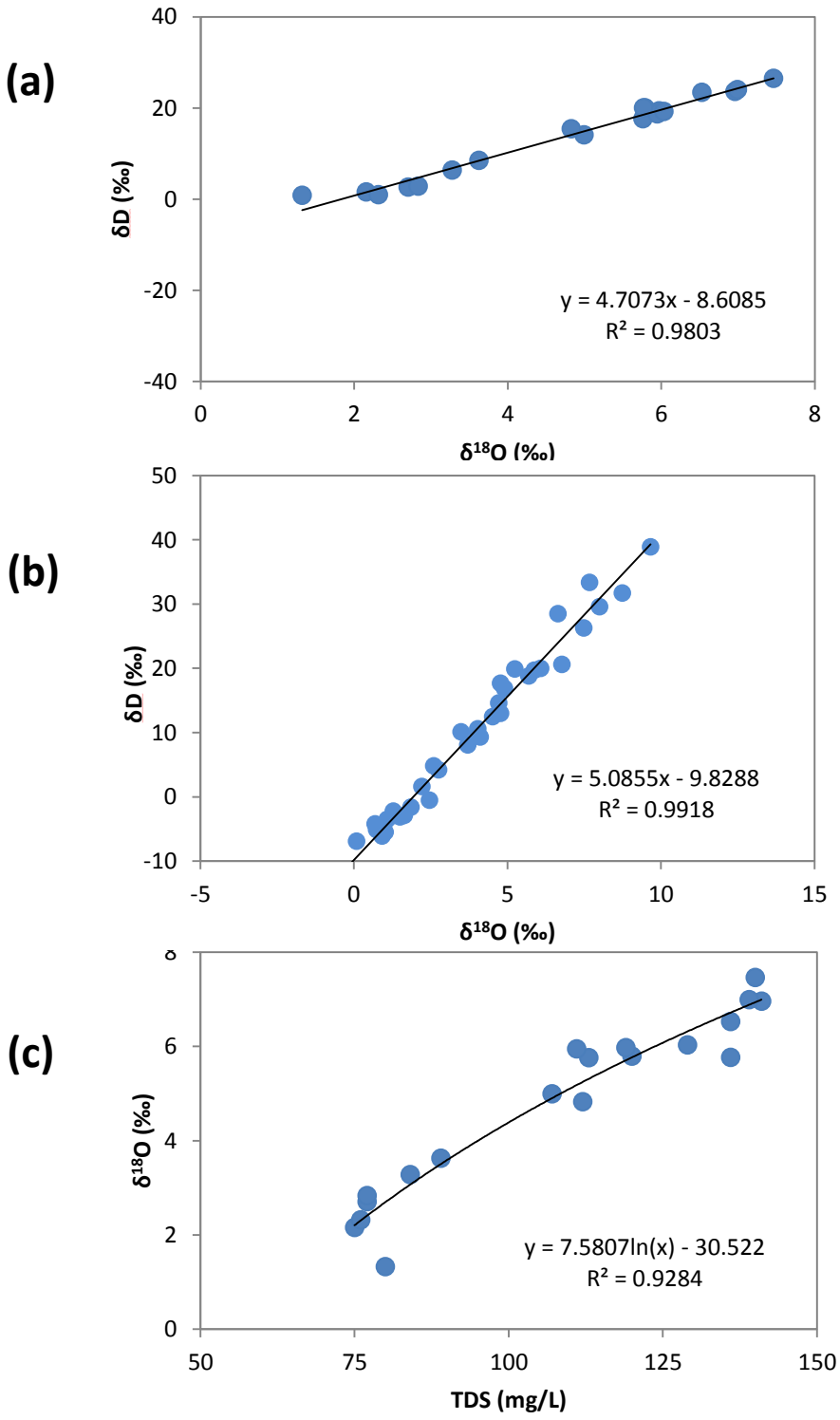

Fig. 4. Cross plots of (a) $\delta^{18}O$ vs. δD for Lake Ngami and (b) $\delta^{18}O$ vs. δD for the Okavango Delta and (c) $\delta^{18}O$ vs. TDS for Lake Ngami.

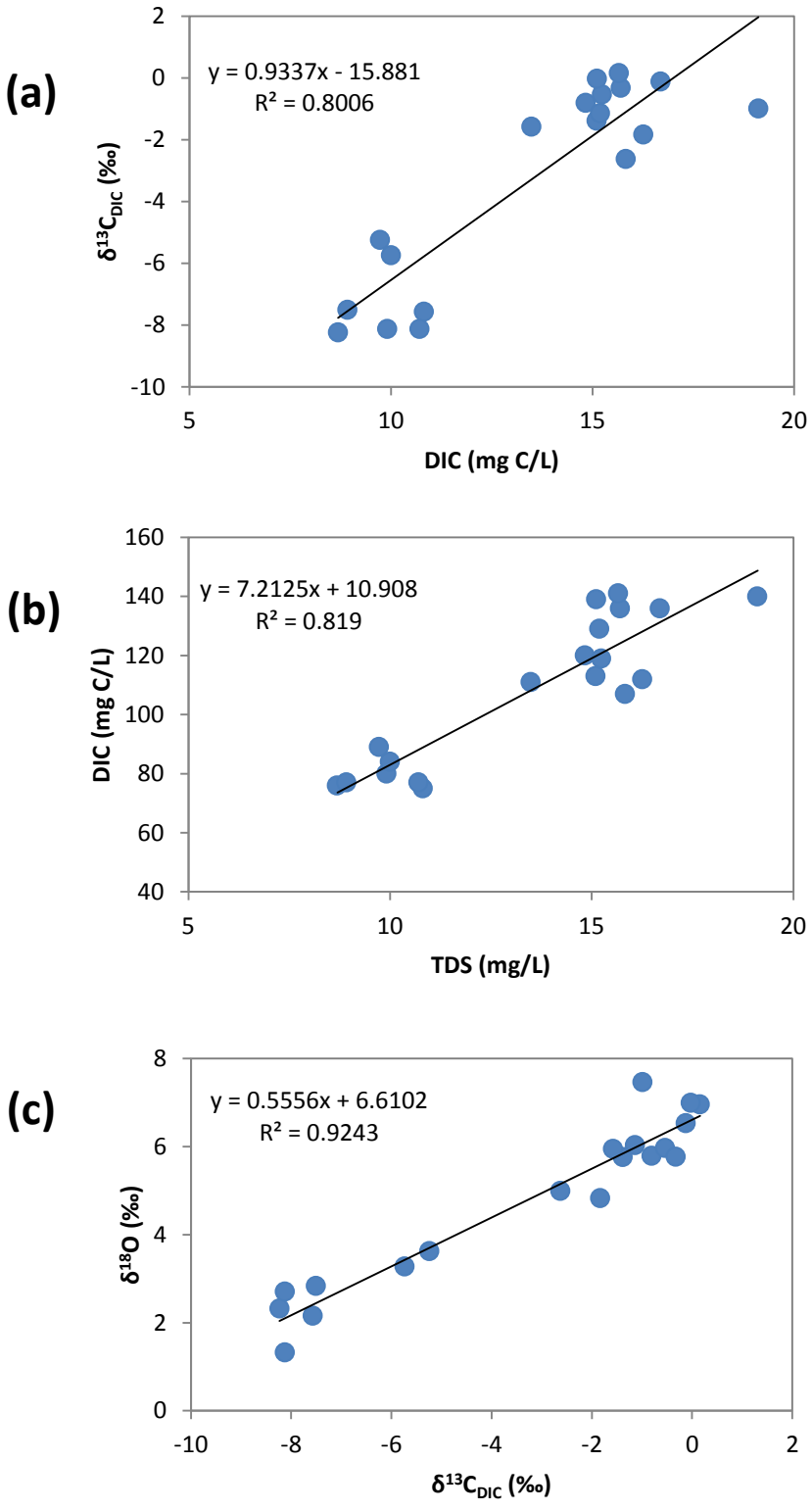

Fig. 5. Cross plots of (a) DIC vs. $\delta^{13}C_{DIC}$ and (b) TDS vs. DIC and (c) $\delta^{13}C_{DIC}$ vs. $\delta^{18}O$.

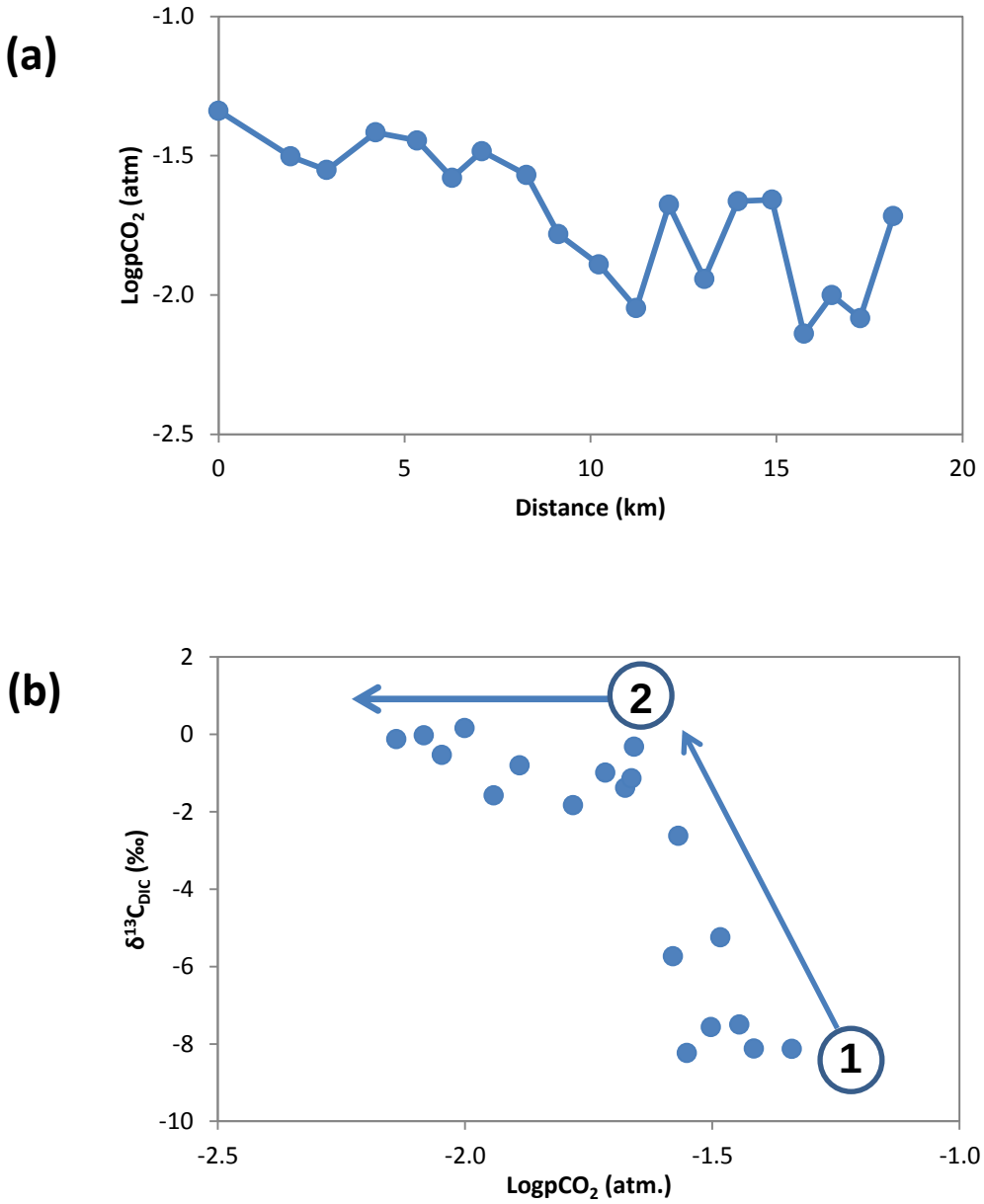

Fig. 6. (a) Plot of the log of the partial pressure of CO_2 (log pCO_2) vs. distance and (b) log pCO_2 vs. $\delta^{13}C_{DIC}$.

Table 1. Physical, chemical, and isotopic results measured along the longitudinal transect of Lake Ngami and in the two inflow rivers.

Distance from point 1 (km)	Water depth (m)	Secci depth (m)	Temperature (°C)	TDS (mg/L)	pH	O_2 (mg/L)	HCO_3^- (mg/L)	Na^+ (mg/L)	K^+ (mg/L)	Mg^{2+} (mg/L)	Ca^{2+} (mg/L)	NH_4^+ (mg/L)	Cl^- (mg/L)	SO_4^{2-} (mg/L)	NO_3^- (mg/L)
0	0.50	-	16.82	80	6.98	7.60	67	9.74	5.31	2.94	10.44	0.23	1.23	0.079	0.29
1.94	1.00	0.75	14.51	75	7.20	7.51	64	9.17	4.77	2.90	9.99	0.23	1.01	0.070	0.18
2.91	1.65	0.70	14.43	76	7.15	7.93	65	9.05	4.77	2.86	10.04	0.19	1.07	0.083	0.29
4.22	2.50	0.90	14.00	77	7.09	6.76	65	9.01	4.79	2.87	9.85	0.34	1.07	0.074	0.34
5.34	3.30	0.90	13.95	77	7.03	7.80	62	9.39	5.06	2.98	10.66	0.23	1.09	0.098	0.30
6.28	3.75	0.88	14.47	84	7.25	8.75	70	9.91	5.69	3.19	10.93	0.25	1.27	0.094	0.39
7.08	3.60	0.85	13.87	89	7.12	8.96	74	10.41	6.15	3.33	11.46	0.42	1.35	0.096	0.31
8.28	3.85	0.75	14.27	107	7.45	6.87	88	11.80	7.78	4.08	14.15	0.26	1.87	0.138	0.39
9.14	3.55	0.80	14.31	112	7.69	9.21	94	12.19	8.51	4.40	15.14	0.28	2.00	0.113	0.22
10.22	3.65	0.75	14.18	120	7.76	7.40	98	12.65	9.13	4.69	16.37	0.18	2.14	0.132	0.18
11.23	3.62	0.75	13.58	119	7.93	9.61	101	12.81	9.25	4.76	16.49	0.25	2.19	0.124	0.24
12.11	3.25	0.78	13.50	113	7.54	9.71	98	12.31	8.71	4.49	15.52	0.21	2.01	0.100	0.30
13.06	3.60	0.75	13.46	111	7.77	9.82	98	12.32	8.78	4.53	15.67	0.21	2.11	0.080	0.23
13.96	3.45	0.78	13.67	129	7.53	8.16	98	12.52	8.93	4.61	16.00	0.30	2.04	0.081	0.00
14.88	3.60	0.70	13.76	136	7.54	9.81	110	12.99	9.50	4.88	17.37	0.29	2.27	0.097	0.38
15.74	3.60	0.80	14.69	136	8.07	9.10	112	13.10	9.87	5.06	17.58	0.29	2.63	0.092	0.33
16.49	3.10	0.72	14.21	141	7.90	9.75	115	13.73	10.48	5.37	18.73	0.23	2.47	0.069	0.23
17.25	2.98	0.68	14.64	139	7.97	7.12	116	13.57	10.46	5.32	19.94	0.20	2.42	0.064	0.33
18.14	2.00	0.60	14.07	140	7.69	9.28	130	14.76	11.68	5.95	20.65	0.35	2.62	0.060	0.27

Table 1. continued

Distance from point 1	CBE	Si SiO_2	Si $CaMg(CO_3)_2$	Si $CaCO_3$	$\delta^{18}O$	δD	DIC	$\delta^{13}C_{DIC}$	$LogpCO_2$	DOC	TN	$\delta^{13}C_{POC}$	$NH_4^+ + NO_3^-$	Inorganic N
(km)	(%)				(‰)	(‰)	(mg C/L)	(‰)	(atm)	(mg/L)	(mg/L)	(‰)	(mg/L)	(%)
0	8.22	-0.34	-3.58	-1.63	1.32	0.88	9.9	-8.1	-1.34	16.45	2.20	-24.22	0.52	23.67
1.94	8.34	-0.43	-3.31	-1.48	2.16	1.60	10.8	-7.6	-1.50	-	-	-	-	-
2.91	6.93	-0.40	-3.40	-1.52	2.32	0.99	8.7	-8.2	-1.55	-	-	-	-	-
4.22	6.87	-0.41	-3.54	-1.60	2.70	2.67	10.7	-8.1	-1.42	-	-	-	-	-
5.34	11.19	-0.36	-3.65	-1.64	2.83	2.86	8.9	-7.5	-1.45	-	-	-	-	-
6.28	8.28	-0.36	-3.06	-1.36	3.28	6.36	10.0	-5.7	-1.58	15.36	1.91	-29.09	0.64	33.52
7.08	7.83	-0.34	-3.25	-1.45	3.62	8.53	9.7	-5.2	-1.48	-	-	-	-	-
8.28	8.29	-0.33	-2.28	-0.97	5.00	14.13	15.8	-2.6	-1.57	-	-	-	-	-
9.14	8.19	-0.35	-1.69	-0.67	4.83	15.43	16.3	-1.8	-1.78	-	-	-	-	-
10.22	8.63	-0.38	-1.46	-0.55	5.79	20.05	14.8	-0.8	-1.89	-	-	-	-	-
11.23	8.05	-0.39	-1.12	-0.38	5.97	19.34	15.2	-0.5	-2.05	24.89	3.09	-28.19	0.48	15.63
12.11	6.62	-0.42	-1.96	-0.80	5.76	17.67	15.1	-1.4	-1.68	-	-	-	-	-
13.06	6.93	-0.39	-1.50	-0.57	5.95	18.73	13.5	-1.6	-1.94	-	-	-	-	-
13.96	8.11	-0.31	-1.95	-0.80	6.03	19.21	15.2	-1.1	-1.66	22.15	2.57	-27.79	0.30	11.52
14.88	5.33	-0.33	-1.78	-0.71	5.77	20.07	15.7	-0.3	-1.66	-	-	-	-	-
15.74	5.48	-0.33	-0.66	-0.16	6.53	23.47	16.7	-0.1	-2.14	-	-	-	-	-
16.49	6.91	-0.30	-0.94	-0.30	6.96	23.66	15.7	0.2	-2.00	-	-	-	-	-
17.25	7.45	-0.33	-0.75	-0.19	6.99	24.01	15.1	0.0	-2.08	-	-	-	-	-
18.14	5.91	-0.41	-1.19	-0.42	7.46	26.53	19.1	-1.0	-1.72	22.81	2.98	-27.15	0.35	20.69

CBE – Charge Balance Error *Si* – Saturation Index

APPENDICES

Appendix A. Field Notes

July 6, 2012 Initial lake sampling

Objective: Travel by boat down the Nhabe River into Lake Ngami to collect samples and conduct a survey along a longitudinal transect of the lake.

We launched our boat from the bridge over the Nhabe River south of Toteng, which is just above the confluence of the Nhabe and Kunyere Rivers. Both adjacent to and beyond the bridge at Toteng, large trucks are observed pumping water from the river, presumably for local mining operations. We also observed dying vegetation, most notably trees, within the flooded river channel. Although the trees completely lack foliage, the limbs are still attached. It is hypothesized that abnormally high floods within this region of the Okavango Delta are encroaching on the areas that commonly are not affected by occasional flooding. This intensified flooding activity is drowning the established dry climate vegetation. We continued approximately 12 km down the river until we reached our first pre-determined sample station 0.5 km before the river flows into Lake Ngami. At this point, samples were collected and physical parameters measured. After sampling we continued downstream toward Lake Ngami. Upon reaching the entrance of the lake, the water was very shallow and the boat was not able to cross large deposits of sand. We could not proceed further and abandoned the survey.

July 19, 2012

Objective: Travel by boat down the Nhabe River into Lake Ngami to complete the previously attempted longitudinal survey.

1. Downriver

We launched from the same location as on July 6th and traveled to the entrance of Lake Ngami. At this time, the flood level had increased in the lower region of the Okavango

Delta. We travel 12.5 – 13 km downstream to the entrance of Lake Ngami. When traveling downstream, the river channel transitions from a wide and shallow channel, to a more confined and deep profile. As we approach the entrance to the lake, dead vegetation along the channel becomes increasingly prevalent (Appendix II, Fig. 3). Large deposits of sand are present at the lake's entrance but we wade in the river and push the boat through the shallow water (Appendix II, Fig. 4).

2. Within the Lake

Upon entering the lake, there are reeds and grasses along with some small trees (Appendix II, Fig. 5-7). Hippos are present in this region of the lake. The vegetated area continues until about 4 km along our survey, at which point the lake becomes an open water body. We direct the survey by GPS and continue to collect samples and physical measurements at pre-determined locations roughly every 1 km. As we travel through the center of the lake the water is vast and open (Appendix II, Fig. 11). It is not until the last sampling stations of our transect that we encounter dead vegetation again (Appendix II, Fig. 12). There are also floating fishing nets in this portion of the lake. Dead vegetation reappears in the space between survey points 17 and 18, but differs from the grasses and trees at the beginning of our transect. At this end of the lake there are no grasses or reeds and the trees that are present have shed the majority of their limbs, indicating that the region has been exposed to flooding for a greater amount of time than the entrance area of the lake.

Appendix B. Field Photos

Figure 1. Nhabe River looking upstream to the bridge at Toteng (20°21’54.2” S; 22°57’18.2” E).

Figure 2. Water pumping adjacent to the Nhabe River approximately 0.5 km downstream from the bridge at Toteng .

Figure 3. Traveling downstream from Toteng to Lake Ngami approximately 12.5 km from the bridge at Toteng.

Figure 4. W. Rutelonis pulling the boat over sand deposits at the entrance to Lake Ngami approximately 13 km downstream from the bridge at Toteng.

Figure 5. Entering Lake Ngami approximately 13.25 km downstream from the bridge at Toteng.

Figure 6. View of dying trees along with reeds and grasses seen when proceeding into Lake Ngami approximately 13.75 km downstream from the bridge at Toteng.

Figure 7. Continuing into Lake Ngami through vegetated margin that surrounds the lake approximately 14.5 km downstream from the bridge at Toteng. Trees pictured are located at sample station 2.

Figure 8. Marginal vegetation along the NW shore of Lake Ngami approximately 15 km downstream from the bridge at Toteng.

Figure 9. Sampling and recording measurements along the beginning of the transect. Looking back toward the inflow river from trees in Figure 7.

Figure 10. Re-entering the vegetated region that surrounds lake Ngami at the conclusion of our survey approximately 13.5 km downstream from the bridge at Toteng.

Figure 11. View of lake Ngami looking SW approximately 20 km downstream from the bridge at Toteng.

Figure 12. Entering vegetation at the distal end of the lake as we approach the end of our survey approximately 29.5 km downstream from the bridge at Toteng.

Appendix C. Additional Data

Table 1. Physical, and chemical measurements along the longitudinal transect of Lake Ngami. Included are measurements taken at 25 cm depth (shallow), and ≈5 cm above the lake bottom (deep).

Distance from point 1	Latitude	Longitude	Temperature	pH	Conductivity		TDS	Oxidation reduction potential		Silica
			deep	deep	shallow	deep	deep	shallow	deep	shallow
(km)			(°C)		(µS/cm)		(mg/L)	(mV)		(mg/L)
0	20° 23' 40.9" S	22° 52' 43.4" E	-	-	123	-	-	-90.2	-	45.5
1.94	20 24' 28.1" S	22 52' 0.3" E	-	-	116	-	-	-98.3	-	35.3
2.91	20° 24' 49.5" S	22° 51' 36.9" E	-	-	117	-	-	-93.9	-	38.2
4.22	20° 25' 18.9" S	22° 51' 3.5" E	13.95	6.95	118	124	0.081	-89.2	-89.1	36.6
5.34	20° 25' 49.4" S	22° 50' 40.9" E	14.65	7.02	119	119	0.077	-93.4	-91.7	41.2
6.28	20° 26' 14.2" S	22° 50' 22.1" E	13.81	6.73	129	145	0.094	-94.3	-91.9	41.2
7.08	20° 26' 40.0" S	22° 50' 14.1" E	13.75	6.69	137	158	0.103	-93.6	-90.4	42.5
8.28	20° 27' 3.5" S	22° 49' 39.0" E	13.65	6.84	165	179	0.116	-96.0	-92.4	44.2
9.14	20° 27' 23.0" S	22° 49' 14.3" E	13.62	6.91	173	186	0.121	-95.9	-89.9	42.9
10.22	20° 27' 43.1" S	22° 48' 45.0" E	13.47	7.06	184	200	0.129	-99.5	-95.4	39.8
11.23	20° 28' 3.4" S	22° 48' 15.0" E	13.34	6.76	183	177	0.115	-105.5	-89.0	38.7
12.11	20° 28' 19.3" S	22° 47' 48.1" E	13.35	7.23	173	175	0.114	-89.7	-92.0	35.4
13.06	20° 28' 36.5" S	22° 47' 22.0" E	13.56	6.82	171	216	0.140	-93.5	-92.8	38.4
13.96	20° 28' 55.5" S	22° 46' 55.6" E	13.51	6.95	198	198	0.129	-86.9	-86.8	45.4
14.88	20° 29' 10.2" S	22° 46' 28.0" E	14.09	6.48	209	344	0.224	-98.0	-112.9	44.2
15.74	20° 29' 22.9" S	22° 46' 0.6" E	14.17	6.87	209	305	0.198	-93.5	-98.5	45.0
16.49	20° 29' 30.7" S	22° 45' 33.7" E	14.03	6.86	216	236	0.153	-89.3	-96.1	47.9
17.25	20° 29' 34.8" S	22° 45' 2.5" E	14.13	6.8	213	260	0.170	-89.8	-97.1	44.6
18.14	20° 29' 43.1" S	22° 44' 31.0" E	14.05	7.17	216	216	0.140	-88.6	-85.1	36.4

VITA

Scott David Meier

Candidate for the Degree of

Master of Science

Thesis: INVESTIGATING THE PROCESSES THAT CONTROL WATER CHEMISTRY DURING REFILLING OF LAKE NGAMI IN SEMIARID NORTHWEST BOTSWANA

Major Field: Geology

Biographical:

Education:

Completed the requirements for the Master of Science in Geology at Oklahoma State University, Stillwater, Oklahoma in May, 2014.

Completed the requirements for the Bachelor of Science in Geology at Arkansas Tech University, Russellville, AR in 2012.

Experience:

-Teaching Assistant - Mineralogy & Petrology; Fall 2012 – Spring 2014; Oklahoma State University, Stillwater, OK

-Society of Exploration Geophysicists Seismic Research; August 2013; Oklahoma State University, Stillwater, OK

-National Science Foundation Research - International research in Botswana; Summer 2012; Oklahoma State University, Stillwater, Ok

-Teaching Assistant - Earth Science and Geology; Fall 2011 – Spring 2012; Arkansas Tech University, Russellville, AR

-Research Assistant - Lake sedimentation modeling; Fall 2010 – Spring 2011; Arkansas Tech University, Russellville, AR

Professional Memberships:

American Association of Petroleum Geologists, American Geophysical Union,

American Institute of Professional Geologists, Geological Society of America